

# Nitrogen air lasing induced by multiple filaments array\*

ZHU Di<sup>1,2</sup>, LI Chunhua<sup>1,2</sup>, GAO Zhongkun<sup>1,3</sup>, SUN Xiaodong<sup>1,2\*\*</sup>, and GAO Hui<sup>4</sup>

1. Tianjin Key Laboratory of Optoelectronic Detection Technology and Systems, Tianjin 300387, China

2. School of Electronics and Information Engineering, Tiangong University, Tianjin 300387, China

3. School of Life Science, Tiangong University, Tianjin 300387, China

4. School of Physical Science and Technology, Tiangong University, Tianjin 300387, China

(Received 4 December 2021; Revised 23 January 2022)

©Tianjin University of Technology 2022

Air lasing emission by launching intense ultrafast laser pulses in atmosphere has recently attracted increasing interest in the ultrafast laser science and atmospheric science fields, especially for remote sensing techniques. We demonstrated the fluorescence emissions at 337 nm, 357 nm and 391 nm induced by multiple filaments using four kinds of step phase plates. Our results have indicated that the fluorescence signal has been amplified as it propagates along the filament through amplified spontaneous emission (ASE), and the fluorescence intensity is also enhanced in the backward direction via multiple filaments. Furthermore, the gain coefficient through ASE is increased with the number of filaments.

**Document code:** A **Article ID:** 1673-1905(2022)06-0354-6

**DOI** <https://doi.org/10.1007/s11801-022-1182-y>

In recent years, ultrafast laser filamentation has drawn more and more interest in the ultrafast laser science and atmospheric science fields. Ultrafast laser filamentation is a special nonlinear optical phenomenon that occurs during the propagation of high power ultrafast laser in transparent optical media<sup>[1-5]</sup>. It is mainly caused by the dynamic interplay of the optical Kerr effect induced self-focusing and defocusing effects of the plasma generated by a high intensity laser or higher-order-Kerr-effect (HOKE)<sup>[6,7]</sup>. Ultrafast laser filamentation is characterized by the critical power for self-focusing at which the self-focusing can overcome the natural diffraction of the laser beam. Under practical experimental conditions, multiple filaments can be found when the peak laser power is much higher than the critical power for self-focusing. Fruitful interaction dynamics, including propelling, attraction, merging, self-steepening, and energy exchanging, etc.<sup>[8-12]</sup>, can be observed during the multi-filamentation propagation. It has many applications in the fields of molecular alignment<sup>[13]</sup>, harmonics of the fundamental beam<sup>[3]</sup>, and terahertz generation<sup>[14,15]</sup>.

Recently, several studies demonstrated that population inversion of  $N_2$  and  $N_2^+$  can be attained in filaments, and optical gain can be achieved<sup>[16,17]</sup> known as “air lasing”. Air lasing emission by filaments has shown considerable potential in the atmospheric remote-sensing applications<sup>[18,19]</sup>. Neutral nitrogen ( $N_2$ ) molecules are promoted to excited states during ultrafast laser pulse filamentary

propagation in atmosphere, leading to a characteristic ultraviolet fluorescence. LUO et al<sup>[20]</sup> reported the presence of backward stimulated emission from filament via 800 nm femtosecond pulses in air, based on an exponential increase of  $N_2$  fluorescence with filament length. They attributed the dependence of the signal intensity to amplified spontaneous emission (ASE). Some researchers also demonstrated air lasing emission by filament utilizing the additional seeding femtosecond laser beam with appropriate wavelengths<sup>[21,22]</sup>.

In this paper, we investigate the behaviors of  $N_2$  air lasing emission by multiple filaments. We demonstrate the fluorescence emissions from the second positive band system  $C^3\Pi_u \rightarrow B^3\Pi_g$  transitions of  $N_2$  at 337 nm (0,0) and 357 nm (0,1) and from the first negative band system  $B^2\Sigma_u^+ \rightarrow X^2\Sigma_g^+$  transitions of  $N_2^+$  at 391 nm (0,0) induced by multiple filaments. The ultrafast laser filamentation array process formed in air via the step phase plate with  $\pi$  phase lag (semi-circular, quarter-circle, six-sextant and eight-octant phase plates). The backscattered fluorescence signal from  $N_2$  molecules demonstrated an exponential increase with the filament length. Our results have indicated that the fluorescence signal has been amplified through ASE as it propagates along the filament. In the meantime, fluorescence intensity is enhanced in the backward direction by multiple filaments. Furthermore, the gain coefficient through ASE is increased with the number of filaments. This is very beneficial for the

\* This work has been supported by the National Natural Science Foundation of China (No.61605144), the Natural Science Foundation of Tianjin City (No.17JCQNJC02000), the Tianjin Municipal Education Commission Program (No.2017KJ099), and the Undergraduate Innovation and Entrepreneurship Training Program of Tiangong University (No.202010058106).

\*\* E-mail: sunxiaodong@tiangong.edu.cn

remote sensing techniques.

The experimental design is illustrated in Fig.1. During the experiment, a 1 kHz, 800 nm, 50 fs full width at half maximum (*FWHM*) Ti: sapphire laser pulse was focused by an  $f=30$  cm lens and step phase plates in air. The phase plate was used to introduce multiple filaments. The initial beam diameter is approximately 1 cm ( $1/e^2$ ). Two dielectric mirrors for 800 nm were employed to reflect the beam at a  $45^\circ$  incident angle. Near the geometrical focus, the multiple filaments were generated by the phase plate. The backscattered fluorescence spectral signal from the multiple filamentations formed in air was then detected using a grating spectrometer (Shamrock 303i, Andor) with a grating at 1 200 grooves per millimeter. The fluorescence spectral signal was collected into the grating spectrometer using a fiber head. In this case, a focal lens 2 ( $f=90$  mm, diameter of 75 mm) was used to couple the fluorescence light into the fiber head.

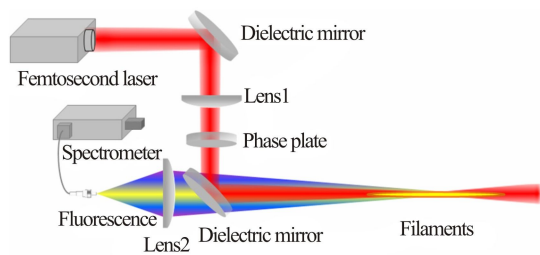


**Fig.1 Experimental design**

Four types of step phase plates called the semi-circular phase plate (SCPP), quarter-circle phase plate (QCPP), six-sextant phase plate (SSPP) and eight-octant phase plate (EOPP) were used to create multiple filaments in our experiment as shown in Fig.2. They are all approximately 1.6 mm in depth and 10 mm in width. The phase plates were divided into 2, 4, 6 and 8 parts, respectively. Between two adjacent parts, each phase plate induced  $\pi$  phase lag at an 800 nm wavelength.

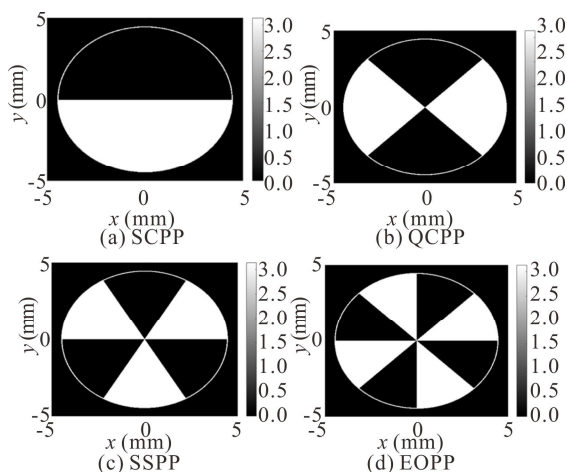


**Fig.2 Schematic diagrams of the phase plates**

Fig.3 depicts the backward fluorescence spectrum of air induced by femtosecond laser filamentation in the range of 320—400 nm. The fluorescence spectrum was obtained by focusing the pump power without phase plate at 1.1 mJ laser energy in the atmosphere. Fig.3 shows that the fluorescence emission via femtosecond laser filamentation is very clean. The fluorescence signals at 337 nm, 357 nm and 391 nm are higher than other wavelengths. The spectral bands have been attributed to the first negative band system  $B^2\Sigma_u^+ \rightarrow X^2\Sigma_g^+$  transitions of  $N_2^+$  and the second positive band system  $C^3\Pi_u \rightarrow B^3\Pi_g$  transitions of  $N_2$ <sup>[23]</sup>. During the femtosecond laser filamentation, multiphoton/tunnel ionization of inner-valence electrons of neutral  $N_2$  molecules was induced by the intense ultrafast laser left the molecular ion  $N_2^+$  in the excited state  $B^2\Sigma_u^+$ , resulting in the fluorescence from the first negative band system  $B^2\Sigma_u^+ \rightarrow X^2\Sigma_g^+$  transitions of  $N_2^+$ . However, the reason for excited state  $C^3\Pi_u$  remains controversial. XU *et al*<sup>[24,25]</sup> reported that the primary  $N_2^+ + N_2 = N_4^+$  reaction followed by the recombination  $N_4^+ + e = N_2 + N_2(C^3\Pi_u)$  is responsible for populating the electronic excited state  $C^3\Pi_u$  of  $N_2$ . The numbers in the parentheses (*v-v*) represent the upper and lower electronic states' vibrational levels. The fluorescence emission lines located at 337 nm, 357 nm and 391 nm are assigned to bands (0,0), (0,1) of the  $N_2$  system  $C^3\Pi_u \rightarrow B^3\Pi_g$  transitions, and band (0,0) of the  $N_2^+$  system  $B^2\Sigma_u^+ \rightarrow X^2\Sigma_g^+$  transitions, respectively.

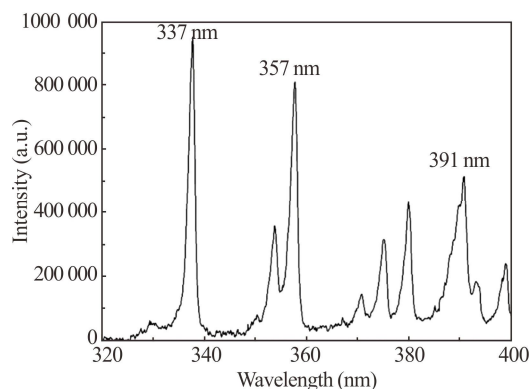


**Fig.3 Typical fluorescence spectral signal induced by femtosecond laser filamentation in the backward direction**

During the experiment, the multiple filaments started before the geometrical focus. We measured the intensity of the fluorescence spectrum that occurred at various laser energies using the four types of step phase plates. To compare the results, we also measured the fluorescence intensity without the step phase plates in the atmosphere. Fig.4 depicts the fluorescence intensities versus filament length at 10 different input energies of 0.5 mJ, 0.88 mJ, 1.1 mJ, 1.3 mJ, 1.47 mJ, 1.62 mJ, 2.05 mJ, 2.38 mJ, 2.49 mJ and 2.59 mJ, respectively. The length of multiple filaments is defined by taking the difference between the self-focusing position of peak power

and the geometrical focusing of the external lens<sup>[20]</sup>. When the input laser energy is lower than a certain value, the fluorescence spectrum signals are too weak to be detected. Thus, the data do not extend to the zero filament length in Fig.4.

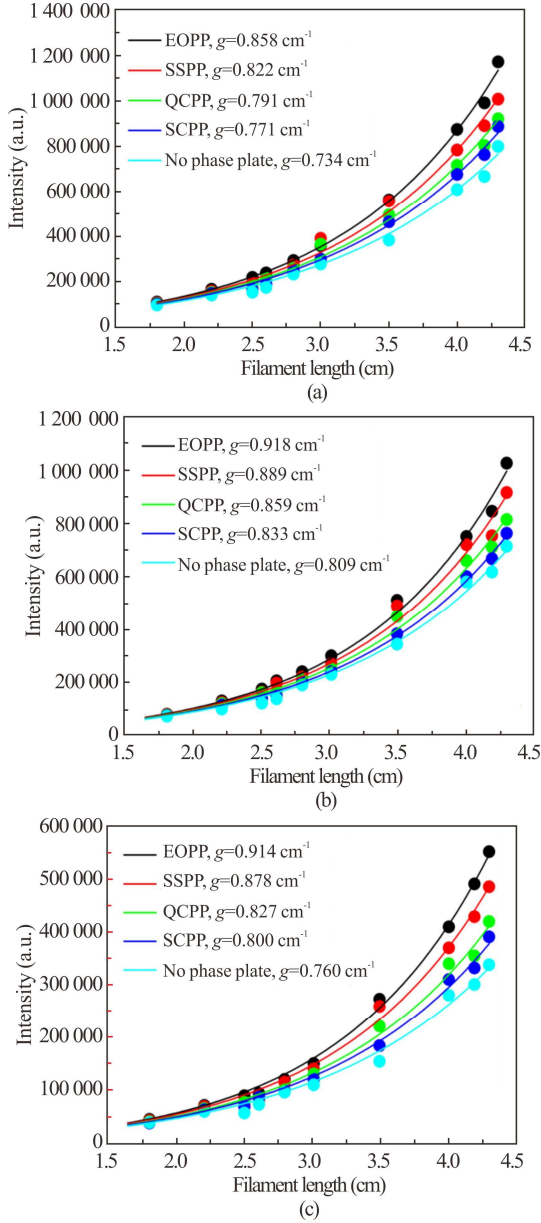


**Fig.4 Fluorescence intensity of N<sub>2</sub> versus the filament length in various types of step phase plates at (a) 337 nm, (b) 357 nm, and (c) 391 nm**

According to LUO et al<sup>[20]</sup>, the backward ASE gain can be defined as

$$I \propto P = \int_0^L P_s e^{g l} dl = \begin{cases} \frac{P_s}{g} (e^{gL} - 1), & \text{with amplification} \\ \frac{P_s}{g} \times gL = P_s L, & \text{without amplification } g \rightarrow 0 \end{cases}, \quad (1)$$

where  $P_s$  represents the spontaneous emission power of the unit length,  $L$  is the estimated filament length, and  $g$  denotes the effective gain coefficient. Because of the intensity clamping inside the filament<sup>[26,27]</sup>, we assume the spontaneous emission power  $P_s$  is uniform for each step phase plate.

To study the relationship between the effective gain coefficient and filament length, using  $P_s$  and  $g$  as fitting parameters, we plotted the fitted curves as solid lines. The experimental results shown in Fig.4 demonstrate that the fluorescence intensity's dependence on the filament length is exponential, which is a direct indication of the presence of gain coefficient through ASE. The fitted gain coefficients differ in various types of step phase plates. All of the curves show a similar tendency at 337 nm, 357 nm and 391 nm, although the signal intensity differs in various types of step phase plates. As demonstrated in Fig.4, the gain coefficients are increased by 0.124 cm<sup>-1</sup>, 0.109 cm<sup>-1</sup> and 0.154 cm<sup>-1</sup> from no step phase plate to EOPP at 337 nm, 357 nm and 391 nm respectively.

To obtain the different numbers of filaments array formation using various types of step phase plates, we conducted the numerical simulations of a 2D+1 ( $A(x, y, z)$ ) nonlinear wave equation<sup>[28]</sup> as

$$2ik_0 \frac{\partial A}{\partial z} + \left( \frac{\partial^2}{\partial x^2} + \frac{\partial^2}{\partial y^2} \right) A + 2k_0^2 \Delta n A = 0, \quad (2)$$

where  $A$  denotes the light field amplitude,  $k_0$  represents the wave number of the beam whose central wavelength is 800 nm, and  $\Delta n$  corresponds to the intensity dependent refractive index which includes the optical Kerr effect and plasma defocusing effect induced nonlinear refractive index,

$$\Delta n = \Delta n_{\text{Kerr}} + \Delta n_{\text{plasma}}, \quad (3)$$

where  $\Delta n_{\text{Kerr}} = n_2 I$ , and  $n_2 = 2 \times 10^{-19} \text{ cm}^2/\text{W}$  corresponds to a critical power of 5 GW for self-focusing in atmosphere. Since the number of the multiple filamentation is our main aim, the plasma refractive index involved in a full four dimensional ( $x, y, z, t$ ) model is replaced by an effective negative refractive index in our current model with the following form:

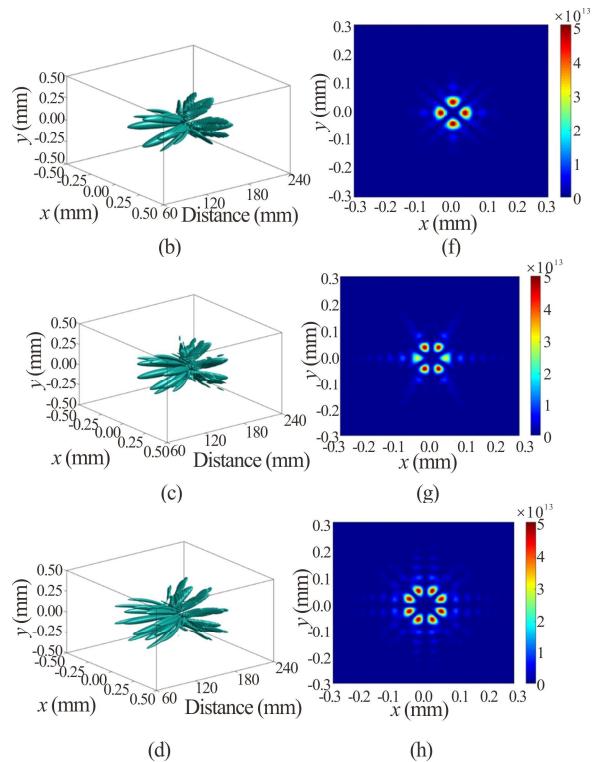
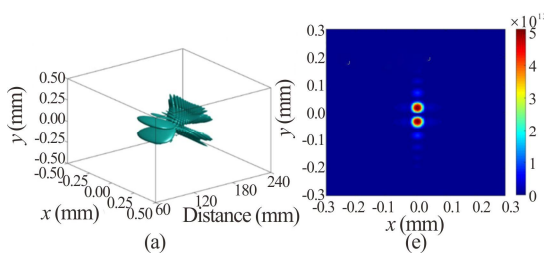
$$\Delta n_{\text{plasma}} = -\sigma I^m, \quad (4)$$

where we set  $m$  equal to 8, which is approximately the reported effective nonlinearity order in air by near infrared femtosecond laser<sup>[29]</sup>.  $\sigma$  is an empirical parameter determined from our previous research, which produces a clamped intensity of  $5 \times 10^{13} \text{ W/cm}^2$ <sup>[30]</sup>.

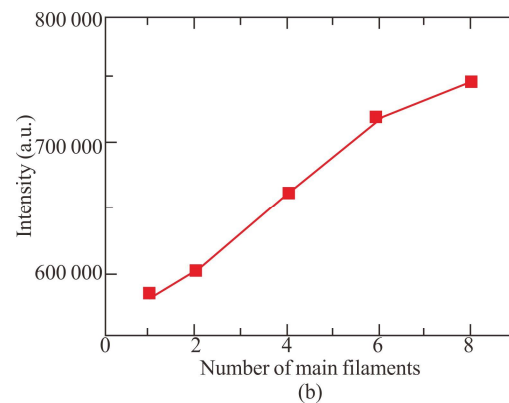
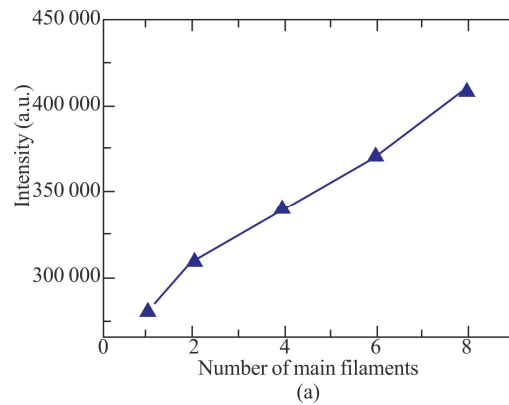
In our simulation, the initial beam profile is formed by Gaussian beams. The input beam radius at the  $1/e^2$  level is 2 mm. To save computation time, the focal length of the lens is set at 15 cm in our simulation. Fig.5(a)–(d) show intensity contours ( $I=1 \times 10^{13} \text{ W/cm}^2$ ) in three-dimensional space during nonlinear propagation when the laser powers are set as 5 times of the critical power for self-focusing with SCPP, QCPP, SSPP and EOPP.

Fig.5(e)—(h) indicate the corresponding laser intensity cross-sectional patterns at the propagation focal distance of  $z=15$  cm. Fig.5 shows the spatial distribution of multiple filaments arrays using the numerical simulation. Multiple filaments were generated using the step phase plates. There are 2, 4, 6 and 8 main filaments in the core and several “child” filaments around them with SCPP, QCPP, SSPP and EOPP, respectively. It can be found that the type of phase plate determines the number and the spatial patterns of filaments array. The femtosecond laser beams passing through the two adjacent parts of the phase plate generated a  $\pi$  phase shift, which divided the laser beam into multiple parts with abrupt phase jump. Each dividing part can independently propagate, resulting in one main filament and several “child” filaments during the nonlinear propagation. The type of phase plate also had an effect on the separation distance between multiple filaments. The numerical simulation coincides well with our previous experimental observation<sup>[12]</sup>.

We further investigate the number of filaments’ dependence of the fluorescence signal at different wavelengths. Fig.6 shows the evolution of the fluorescence signal as a function of the number of main filaments created by different step phase plates at the wavelength of 337 nm, 357 nm and 391 nm, respectively. One main filament is created only by focusing lens without the step phase plates. The 2, 4, 6 and 8 main filaments are created combining SCPP, QCPP, SSPP and EOPP with focusing lens. As shown in Fig.6, all three curves increase significantly with the number of filaments. As previously mentioned, since the excitation and ionization processes for  $N_2$  molecules inside the filament are nonlinear, the possibility of multiphoton ionization to  $N_2^+$  is determined by the number of multiple filaments. This indicates that a higher number of filaments can produce a greater degree of plasma density and fluence distribution. The intense filamentary pulse of peak intensity is high enough to liberate free electrons from  $N_2$  and oxygen molecules through a high-field tunneling process. As a result, the population difference, that is the effective gain coefficient, is directly related to the plasma density, which follows the spatial distribution of multiple filaments. The fluorescence from the different numbers of multiple filaments underwent different amplifications. The experimental results shown in Fig.4 also confirmed our hypothesis. The gain coefficient through ASE is increased with the number of filaments.



**Fig.5 Simulated intensity distributions for use of step phase plates in air: Intensity contours ( $I=1 \times 10^{13} \text{ W/cm}^2$ ) in three-dimensional space during nonlinear propagation with (a) SCPP, (b) QCPP, (c) SSPP, and (d) EOPP when the laser powers are set at 5 times of the critical power for self-focusing; (e)—(h) Transverse distributions at  $z=15$  cm corresponding to (a)—(d), respectively**



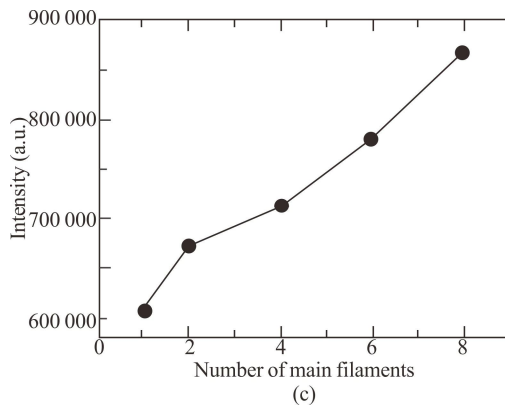


**Fig.6 Fluorescence intensity in air versus the number of main filaments created by different types of step phase plates at (a) 391 nm, (b) 357 nm, and (c) 337 nm**

In conclusion, we have demonstrated that the step phase plate with  $\pi$  phase lag could generate ultrafast laser filament array in air. The fluorescence emissions at 337 nm, 357 nm and 391 nm could be induced by multiple filaments using four types of step phase plates. Our results have indicated that the fluorescence emission is amplified through ASE as it propagates along the filament and the backscattered fluorescence intensity is also enhanced by multiple filaments. Furthermore, the gain coefficient through ASE is increased with the number of filaments. The generation of coherent radiation in the experiments with such cavity-less laser sources holds great potential for remote sensing applications. The high beam quality, stability, and power will allow detection of impurities in air with high sensitivity. This is very beneficial for many applications, such as standoff spectroscopy, pollutant detection, and remote sensing techniques.

### Acknowledgments

We acknowledge Professor LIU Weiwei for his discussions and assistance in setting up this experiment.

### Statements and Declarations

The authors declare that there are no conflicts of interest related to this article.

### References

- [1] CHIN S L, HOSSEINI S A, LIU W, et al. The propagation of powerful femtosecond laser pulses in optical media: physics, applications, and new challenges[J]. Canadian journal of physics, 2005, 83(9): 863-905.
- [2] CHIN S L, THÉBERGE F, LIU W. Filamentation nonlinear optics[J]. Applied physics B, 2007, 86(3): 477-483.
- [3] COUAIRON A, MYSYROWICZ A. Femtosecond filamentation in transparent media[J]. Physics reports, 2007, 441(2-4): 47-189.
- [4] BERGÉ L, SKUPIN S, NUTER R, et al. Ultrashort filaments of light in weakly ionized, optically transparent media[J]. Reports on progress in physics, 2007, 70(10): 1633-1713.
- [5] KASPARIAN J, WOLF J P. Physics and applications of atmospheric nonlinear optics and filamentation[J]. Optics express, 2008, 16(1): 466-493.
- [6] BÉJOT P, KASPARIAN J, HENIN S, et al. Higher-order Kerr terms allow ionization-free filamentation in gases[J]. Physical review letters, 2010, 104(10): 103903.
- [7] BÉJOT P, HERTZ E, KASPARIAN J, et al. Transition from plasma-driven to Kerr-driven laser filamentation[J]. Physical review letters, 2011, 106(24): 243902.
- [8] XI T T, LU X, ZHANG J. Interaction of light filaments generated by femtosecond laser pulses in air[J]. Physical review letters, 2006, 96(2): 025003.
- [9] MA Y Y, LU X, XI T T, et al. Filamentation of interacting femtosecond laser pulses in air[J]. Applied physics B, 2008, 93(2): 463-468.
- [10] SHIM B, SCHRAUTH S E, HENSLEY C J, et al. Controlled interactions of femtosecond light filaments in air[J]. Physical review A, 2010, 81(6): 061803.
- [11] TZORTZAKIS S, BERGÉ L, COUAIRON A, et al. Breakup and fusion of self-guided femtosecond light pulses in air[J]. Physical review letters, 2001, 86(24): 5470-5473.
- [12] GAO H, CHU W, YU G, et al. Femtosecond laser filament array generated with step phase plate in air[J]. Optics express, 2013, 21(4): 4612-4622.
- [13] LI H, LIU J, FENG Y, et al. Temporal and phase measurements of ultraviolet femtosecond pulses at 200 nm by molecular alignment based frequency resolved optical gating[J]. Applied physics letters, 2011, 99(1): 011108.
- [14] WANG T J, DAIGLE J F, YUAN S, et al. Remote generation of high-energy terahertz pulses from two-color femtosecond laser filamentation in air[J]. Physical review A, 2011, 83(5): 053801.
- [15] LI M, LI W, SHI Y, et al. Verification of the physical mechanism of THz generation by dual-color ultrashort laser pulses[J]. Applied physics letters, 2012, 101(16): 161104.
- [16] XU H, LÖTSTEDT E, IWASAKI A, et al. Sub-10-fs population inversion in  $N_2^+$  in air lasing through multiple state coupling[J]. Nature communications, 2015, 6: 8347.
- [17] YAO J, JIANG S, CHU W, et al. Population redistribution among multiple electronic states of molecular nitrogen ions in strong laser fields[J]. Physical review letters, 2016, 116(14): 143007.
- [18] MITRYUKOVSKIY S, LIU Y, DING P, et al. Backward stimulated radiation from filaments in nitrogen gas and air pumped by circularly polarized 800 nm femtosecond laser pulses[J]. Optics express, 2014, 22(11): 12750-12759.
- [19] DOGARIU A, MICHAEL J B, SCULLY M O, et al. High-gain backward lasing in air[J]. Science, 2011,

- 331(6016): 442-445.
- [20] LUO Q, LIU W, CHIN S L. Lasing action in air induced by ultra-fast laser filamentation[J]. *Applied physics B*, 2003, 76(3): 337-340.
- [21] YAO J, ZENG B, XU H, et al. High-brightness switchable multiwavelength remote laser in air[J]. *Physical review A*, 2011, 84(5): 051802.
- [22] YAO J, LI G, JING C, et al. Remote creation of coherent emissions in air with two-color ultrafast laser pulses[J]. *New journal of physics*, 2013, 15(2): 023046.
- [23] BRITTON M, LAFERRIERE P, KO D H, et al. Testing the role of recollision in  $N_2^+$  air lasing[J]. *Physical review letters*, 2018, 120(13): 133208.
- [24] XU H L, AZARM A, BERNHARDT J, et al. The mechanism of nitrogen fluorescence inside a femtosecond laser filament in air[J]. *Chemical physics*, 2009, 360(1-3): 171-175.
- [25] XU H L, AZARM A, CHIN S L. Controlling fluorescence from  $N_2$  inside femtosecond laser filaments in air by two-color laser pulses[J]. *Applied physics letters*, 2011, 98(14): 141111.
- [26] BRAUN A, KORN G, LIU X, et al. Self-channeling of high-peak-power femtosecond laser pulses in air[J]. *Optics letters*, 1995, 20(1): 73-75.
- [27] LIU W, PETIT S, BECKER A, et al. Intensity clamping of a femtosecond laser pulse in condensed matter[J]. *Optics communications*, 2002, 202(1-3): 189-197.
- [28] SKUPIN S, BERGÉ L, PESCHEL U, et al. Filamentation of femtosecond light pulses in the air: turbulent cells versus long-range clusters[J]. *Physical review E*, 2004, 70(4): 046602.
- [29] TALEBPOUR A, YANG J, CHIN S L. Semi-empirical model for the rate of tunnel ionization of  $N_2$  and  $O_2$  molecule in an intense Ti: sapphire laser pulse[J]. *Optics communications*, 1999, 163(1-3): 29-32.
- [30] LIU W, CHIN S L. Abnormal wavelength dependence of the self-cleaning phenomenon during femtosecond-laser-pulse filamentation[J]. *Physical review A*, 2007, 76(1): 013826.